NAT. CROAT. | VOL. 34 | No 1 | 37-51 | ZAGREB | August 31, 2025

original scientific paper / izvorni znanstveni rad
DOI 10.20302/NC.2025.34.4

WEATHERING RATE OF LATE EOCENE CLASTICS OF LOPAR PENINSULA (RAB ISLAND, CROATIA)

Tihomir Marjanac* & Marina Čalogović

ProGEO-Croatia, Horvatovac 102a, 10000 Zagreb, Croatia (independent researchers)

Marjanac, T. & Čalogović, M.: Weathering rate of Late Eocene clastics of Lopar Peninsula (Rab Island, Croatia). Nat. Croat., Vol. 34, No. 1, 37-51, Zagreb, 2025.

The weathering rate of coastal rocks of the islands of the eastern Adriatic is generally unknown, and only qualitatively interpreted after cartographic data from various sources and ages. Herein we present our results of monitoring of weathering of Late Eocene sandstones and sandy marls of which Lopar Peninsula on the Island of Rab in the Northern Adriatic Quarnero Bay are built. The monitoring lasted 4 years and the measured annual weathering rate of sandstonesranges from 0.42 to 1.21 mm, whereas the sandy marls were weathered by 1.54 to 1.55 mm. The measured weathering rate is strongly related to the distance of the measurement polygon from the coastline and splash-zone, and protectedness of the micro locality from abrasion by wind-blown quartz sand. The Lopar sand beaches are fed by quartz sand released from Eocene clastics by weathering, and we have estimated the minimal supply of sand from the area of 100 m^2 in 100 and 1000 years respectively, assuming the modern climate.

Key words: Sandstones, mineralogical composition of sands, sand-blasting, carbonate leaching, Quarnero Bay, coastal retreat, monitoring, geomorphology

Marjanac, T. & Čalogović, M.: Intenzitet trošenja kasno eocenskih klastita poluotoka Lopara (otok Rab, Hrvatska). Nat. Croat., Vol. 34, No. 1, 37-51, Zagreb, 2025.

Intenzitet trošenja obalnih stijena sjevernojadranskih otoka općenito nije poznat, nego se procjenjuje na temelju analize topografskih karata iz različitih izvora i starosti. Ovdje donosimo rezultate našeg monitoringa trošenja eocenskih pješčenjaka i pjeskovitih lapora koji grade poluotok Lopar na otoku Rabu u Kvarnerskom zaljevu. Monitoring je trajao 4 godine, a mjerenja ukazuju na godišnje trošenje pješčenjaka u iznosu od 0,42 do 1,21 mm te pjeskovitih lapora u iznosu od 1,54 do 1,55 mm. Izmjereni intenzitet trošenja jako ovisi o udaljenosti mjerne plohe od obalne linije i zone prskanja te zaštićenosti mikrolokacije od abrazije vjetrom donesenog kvarcnog pijeska. Pješčane plaže na Loparu prihranjuje kvarcni pijesak koji nastaje trošenjem eocenskih klastita, pa smo izračunali i minimalni doprinos trošenja s površine od 100 m^2 u trajanju od 100 i 1000 godina, pod pretpostavkom da je klima bila jednaka današnjoj.

Ključne riječi: pješčenjaci, mineraloški sastav pijeska, pjeskarenje, otapanje karbonata, Kvarnerski zaljev, povlačenje obale, monitoring, geomorfologija

*corresponding author: tihomirmarjanac@gmail.com

INTRODUCTION

Lopar Peninsula on the Northern Adriatic island of Rab in Croatia (Fig. 1) is severely affected by erosion due to its lithological composition and exposure to wind and wave action. The intensity of weathering on Lopar was so far only estimated after study of topographic maps and aerial photographs, which missed quantitative and time-dependent data. To provide quantitative data on weathering rate of Late Eocene clastics on Rab Island we have conducted real-time monitoring over a duration of 4 years. The monitoring comprised successive measurements at 9 locations at different positions relative to distance from the coastline, exposure to wind, and lithological variability (Fig. 2). In this study we revealthe effects of distance from the coastline, the effects of lithological variability and provide estimates on the amount of sand supply for the Lopar beaches.

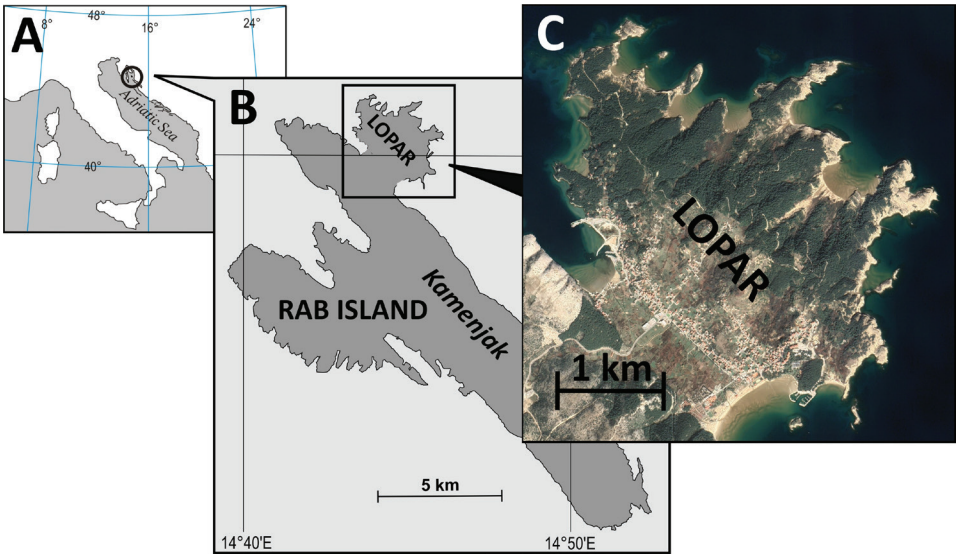

Fig. 1. A) Position of the study area, B) Position of the Lopar Peninsula, C) Topography of the Lopar Peninsula. Google Earth satellite image of 2/2021.

Vulnerability of coasts of Northern Adriatic islands, Rab Island in particular, is of keen interest to several researchers who have based their study on cartography and numerical modelling (e.g. Benac *et al.*, 2006; Ružić & Benac, 2016; Ružić *et al.*, 2023) primarily from the aspect of the possible consequences of sea-level rise and expected increase in the height of waves.

NORTHERN ADRIATIC WIND AND WAVE CLIMATE

The Northern Adriatic Sea, the Quarnero Bay in particular, is affected primarily by the 'bora' wind blowing from the North, Northeast and East. The bora is an anticyclone wind that blows from the coastal mountains in gusts, and can locally reach very high speeds of over 65 m/s. It generates waves that may reach a height of over 4 m, and splash the exposed coasts up to over 10 m above the sea level. The bora is strongly

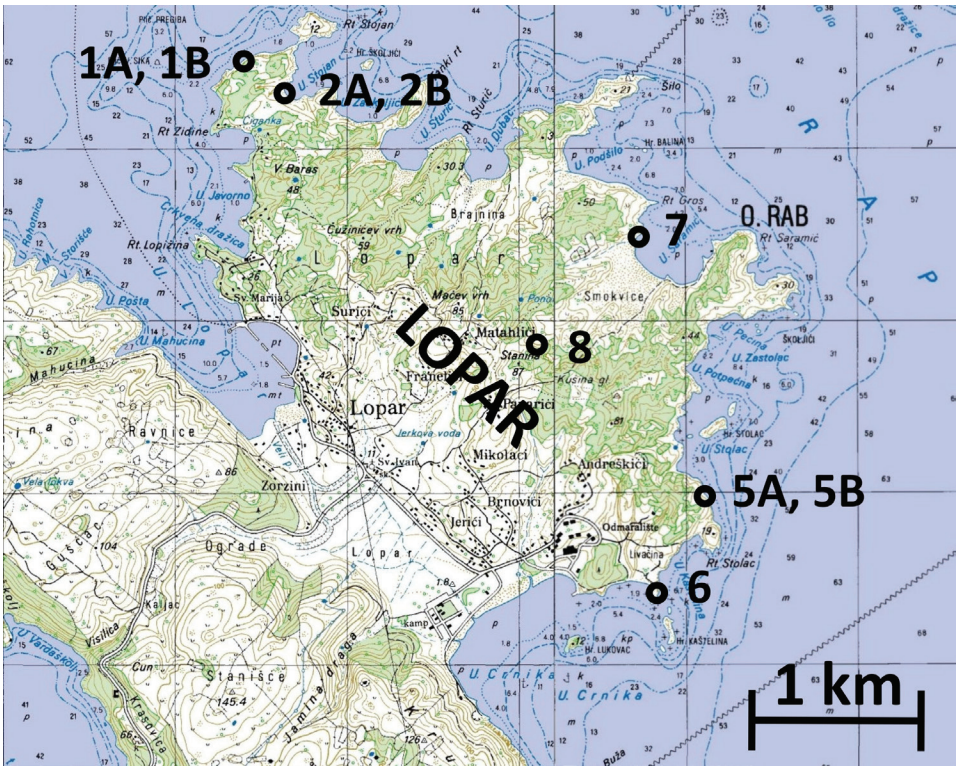

Fig. 2. Locations of the study quadrants. Due to restrictions of the map scale, quadrants 1A and 1B, 2A and 2B, 5A and 5B are not individually labelled.

controlled by topography of the mountainous hinterland, but it also shapes the topography of the inner Adriatic Islands by extensive denudation and salting. The second in terms of frequency of occurrence is the 'sirocco' wind, which blows from Southeast and South along the Eastern Adriatic coast and can reach a speed of 30 m/s, and generate the highest waves in the Adriatic Sea (Katalinić, 2019; Katalinić & Parunov, 2014). Although other winds also blow in the eastern Adriatic Sea, they are subordinate in the study area (Fig. 3), and Lopar Peninsula in particular is topographically well protected from their influence by the main island ridge of Kamenjak. Because of the strong wind and wave action, the northern and eastern coasts of Lopar Peninsula are characterized by deep coves and narrow promontories with cliffs (Fig. 1).

LATE EOCENE CLASTICS OF RAB ISLAND

Rab Island is tectonically built of two anticlines with Cretaceous carbonates in cores and two synclines which host Eocene carbonates and clastics (Fig. 4). The focus of our study was the Eocene clastics in the Lopar syncline, which also occur in the Rab syncline. The quality of exposure is best in the Lopar syncline, with negligible urbanization and anthropogenic influence.

Paleogene deposits of the Rab Island comprise Low-Middle Eocene limestones, usually referred to as foraminiferal limestones which are overlain by the so-called

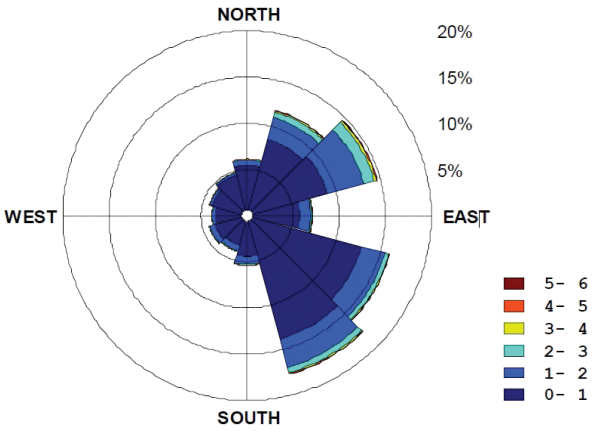

Fig. 3. Windrose for Northern Adriatic Sea, from Katalinić (2019).

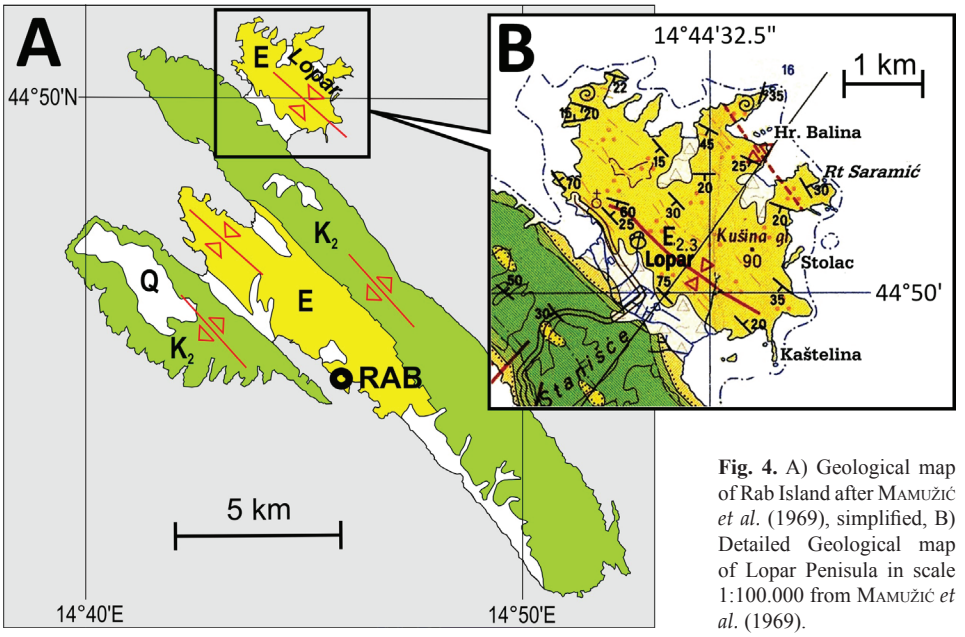

Fig. 4. A) Geological map of Rab Island after Mamužić *et al.* (1969), simplified, B) Detailed Geological map of Lopar Penisula in scale 1:100.000 from Mamužić *et al.* (1969).

transitional beds. These are overlain by thick clastic succession which is referred to as Lower and Upper Flysch (Mamužić, 1962; Mamužić *et al.*, 1969; Mamužić & Milan, 1973) in the old literature. The Lower Flysch unit was later redefined as the San Marino Marls (Marjanac & Marjanac, 1999, 2004), predominantly marly with only thin sand interbeds (Muldini-Mamužić, 1962), whereas the Upper Flysch unit was redefined as Lopar sandstones composed of thick sandstones interbedded with marly intervals (Fig. 5). The focus of our interest was Lopar Sandstones and the rate at which they weather, which has shaped the topography of the Lopar peninsula, characterized by sandy coves and bays, separated by narrow promontories (Figs. 1 and 2).

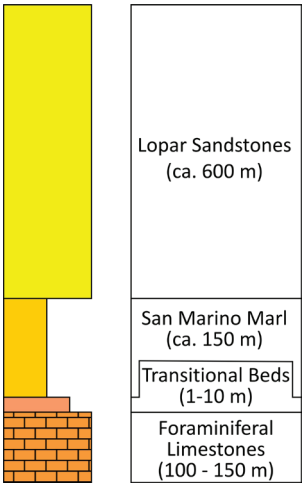

Fig. 5. Simplified stratigraphic column of Lopar Eocene deposits.

Lithology

The Lopar Sandstones unit consists of quartz sandstones and bioturbated sandy marls in alternation, and sporadic thin conglomerate interbeds. The sandstones occur as: i) thin interbeds in marls, ii) as packages of stacked sandstone beds ("sheet sandstones") and iii) as several metre thick sandstone bodies, commonly capped by sandy marls. These three lithologies occur in repetitive succession. The stacked sandstone beds are organized in thickening-upward (progradational) successions, whereas sandstone bodies are internally cross-bedded, and sharply overlain by thin shell-beds made of resedimented *Nummulites* and fragmented bivalves, and capped by bioturbated sandy marls. Conglomerates consist of abundant well rounded chert and quartzite pebbles, rare rounded limestone pebbles, sandstone cobbles and abundant fragmented bivalves. They commonly occur in bases of sandstone bodies, but also as conglomerate interbeds within some sandstones.

Age

The age of the Lopar Sandstones is poorly constrained as Middle - Late Eocene. The lack of indigenous microfossils in sandstones and associated marly sandstones and the great abundance of resedimented foraminifera and macrofossils were recognized by Muldini-Mamužić (1962) who attributed it to the shallowing of the depositional environment. She assigned the Lopar Sandstones to the uppermost Middle Eocene and possibly to a part of the Late Eocene.

Benić (1983) found nannofossils of the NP16 nannozone (Late Lutetian-Earliest Bartonian) in the San Marino Marls, and found a predominance of resedimented forms in the studied Lopar sandstones, so he assumed that they may belong to the same or a younger biozone. Marjanac & Marjanac (2007) interpreted the abundance of resedimented fossils as a consequence of erosion and resedimentation during relative sea-level falls which caused truncation of the underlying sediments. The frequent relative sea-level changes that characterize the deposition of Lopar Sandstones best correlate with Third-order cycles 3.5 to 4.3 of Haq *et al.* (1987) which correspond to a Bartonian - Priabonian time span.

Herein we adopt Late Eocene age of the Lopar Sandstones based on sequence stratigraphic research and recent discovery of Late Eocene - Oligocene the palaeomammal Palaeoamassia in the base of one sandstone body (Lihoreau *et al.*, 2023).

Origin and depositional environment

The provenance of quartz sand, chert and quartzite pebbles was outside of the present Dinaric range, most likely in the far north of the European land mass, and was transported by a large alluvial system. The provenance of rare limestone pebbles was presumably in exposed palaeo-Dinaric Mountains and probably represents erosional remnants of lowstand alluvial deposits.

The sheet sandstones are interpreted in terms of shoreface storm deposits. These are as a rule truncated by the bases of overlying cross-bedded sandstone bodies, which are interpreted as depositional sequence boundaries. Truncation of shoreface deposits is caused by significant relative sea-level falls, and rapid basinward migration of facies. The overlying sandstone bodies have geometry and internal architecture of sandwaves or complex dunes which were deposited by high-amplitude tidal currents in incised valleys or estuaries (Marjanac & Marjanac, 2007) during relative sea-level rises.

The Lopar sandstone bodies are overlain first by shell beds which are interpreted as storm-beds, and these are sharply overlain by sandy marls. This sediment succession was deposited as the rise in the sea level accelerated and flooded the incised valleys and their interfluves.

The Lopar sediment succession documents more than 28 episodes of relative sea level rise and fall (Marjanac & Marjanac, 2007), which are probably 3rd order sequences *sensu* Mitchum and Van Wagoner (1991). Frequent oscillations in relative sea level forced basinward and landward shifts of facies, so we interpret the depositional environments as a wave-dominated paralic sea in periods of high sea-level, and tide-dominated incised valley(s) which were formed during relative sea-level falls and filled during successive rises in the sea level.

METHODS AND PROTOCOLS

This study of weathering of Late Eocene clastics draws on previous geological research into Rab Island geology (Mamužić, 1962; Mamužić *et al.*, 1969; Mamužić & Milan, 1973) and on the sedimentology of Eocene clastics (Marjanac & Marjanac, 2007). For the purpose of this study we have analysed mineralogical and chemical composition of several rock samples from the localities selected for monitoring of the weathering rate by means of optical microscopy, calcimetry and X-Ray diffraction.

For qualitative assessment of the studied rock samples we have applied optical microscopy of standard thin sections stained in a solution of Alizarine Red-S and KFeCN according to the procedure in Bouma (1969). Thin sections were analysed in transmitted light under a Leitz polarizing microscope with and without crossed polars, to obtain data on debris mineralogy (calcite and its variants vs. quartz) and the mineralogy of the bonding cement.

Quantitative assessment of the amounts of calcite and quartz was obtained by X-Ray diffraction of powdered rock debris which was collected during the drilling of measurement boreholes. Drilling provided fine sand and silt powder which needed

only minor additional powderization in agate mortar before application on aluminium holders for X-Ray diffraction analysis. We have used Philips X'Pert Pro diffractometer and the diffractograms were analysed by QualX software package (Altomare *et al.*, 2015), which provided the mineral composition of the analysed samples.

After X-Ray diffraction, the analysed powder was removed from aluminium holders and subjected to calcimetric analysis to reveal the content of $CaCO_3$. About 0.3 g of rock powder was dissolved in 10 ml diluted HCl with a concentration of 2.5% at room temperature for 1 hour. The solution was then filtered, dried and the mass of undissolved residuum on filter-paper was measured on an analytical scale. The mass of undissolved residuum was subtracted from the mass of filter-paper and the value was subtracted from the mass of the analysed sample to obtain the mass of dissolved $CaCO_3$.

Quantitative assessment of weathering rate was performed in the field at 9 sites (Fig. 2), selected to provide data on different lithological variants at different height above the sea-level (from 1 m to 58 m a.s.l.) and different distances from the coastline (within and outside the splash zone) and exposure to prevailing north-eastern and southern winds (Fig. 3). The "exposure of measurement quadrants as used in Tab. 1 refers to the physical orientation of the measurement polygon, not necessarily to the winds blowing only from that direction. Micro-locations of some quadrants (e.g. 1A, 5A, 5B, 6) are topographically protected from winds blowing from their rear because they are mounted on vertical cliff faces.

Tab. 1. Monitoring sites and corresponding quadrants, locations and lithology of substrate

Quadrant	Site coordinates			Exposition	Distance from coastline (m)	Lithology
	X	Y	z (m)			
1A	N44°51'4.35"	E14°43'18.47"	6	W	30	sandstone
1B	N44°51'5.81"	E14°43'19.9"	3	N	15	sandy marl
2A	N44°50'59.5"	E14°43'28.6"	5	NE	50	sandstone
2B*	N44°50'58.0"	E14°43'31.3"	4	NE	30	sandstone
5A	N44°49'44.53"	E14°45'22.27"	4	NE	2	sandy marl
5B	N44°49'44.31"	E14°45'22.25"	12	NE	10	sandstone
6**	N44°49'26.32"	E14°45'10.04"	1	E	2	sandstone
7**	N44°50'33.51"	E14°45'5.65"	1	SW	2	sandstone
8**	N44°50'13"	E14°44'36"	58	NE	685	sandstone
* quadrant mounted in 2019, ** quadrant mounted in 2020						

The rate of weathering was measured on a measurement quadrant with an area of 1 m^2. Each quadrant had 5 boreholes drilled in each corner of a square and one in its centre (Fig. 6A). The rate of weathering was measured as the change in depth of shallow boreholes drilled in the rock face (Fig. 6B).

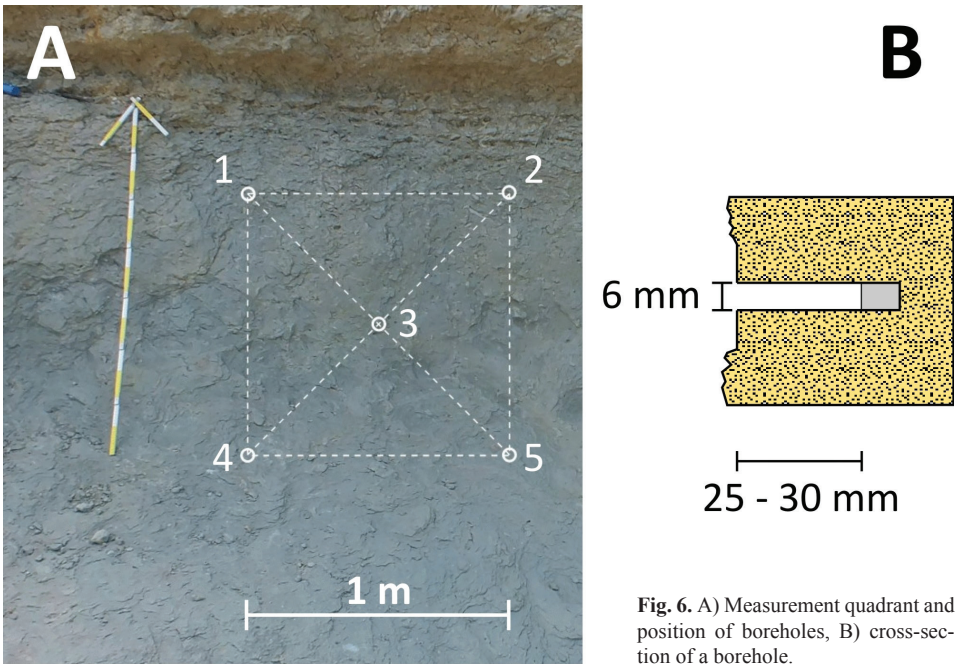

Fig. 6. A) Measurement quadrant and position of boreholes, B) cross-section of a borehole.

A typical borehole was 25 - 30 mm deep, 6 mm in diameter, with a steel plug at the end. The borehole mouth was flattened by milling to minimise micro-topography of the rock face and to assure regular surface for measurement of the borehole depth. Most boreholes were drilled horizontally, perpendicularly to the rock face, except for a few which had to be drilled vertically due to the morphology of the rock face. Each measurement quadrant was marked in the field by identification letter by synthetic spray paint. This painted lettering provided additional information on weathering rate on a larger area.

Boreholes were cleaned with compressed air before each periodic measurement of their depth to remove the accumulated debris and any possible insects which might have nested in them. The depth of each borehole was measured with a precision of 0.01 mm witha hand digital micrometer, and 12 successive measurements were made on each borehole to attain objective data. Average depth and standard deviation of 12 measurements was calculated for each borehole, as well as the difference of initial depth (which was measured by the same procedure during setup of quadrants) and periodic control measurement. These data were used to calculate the average difference in depths for all 5 boreholes on one quadrant. The value for each quadrant indicates the amount of weathered rock in the time between two successive measurement campaigns, and finally after 4 years of successive monitoring.

The monitoring started on 25.3.2018 and ended on 3.11.2022, and comprised 15 successive periodic measurement campaigns, separated by approximately 4 months. Monitoring lasted 1684 days for the measurement sites 1A, 1B, 2A, 5A, and 5B, and 706 days for sites 6, 7 and 8 which were added later. In all, we made 7094 individual measurements of borehole depths.

MATERIALS

Diffractograms of powdered samples from measurement boreholes (Fig. 7, Tab. 2) show the predominance of quartz in all samples, in the range of 68.6 - 77.7 %, and 22.3 - 31.4 % of calcite. Iron was also detected, but with a very low value in sample 2, and at the detection limit in samples 1B, 5A and 5B.

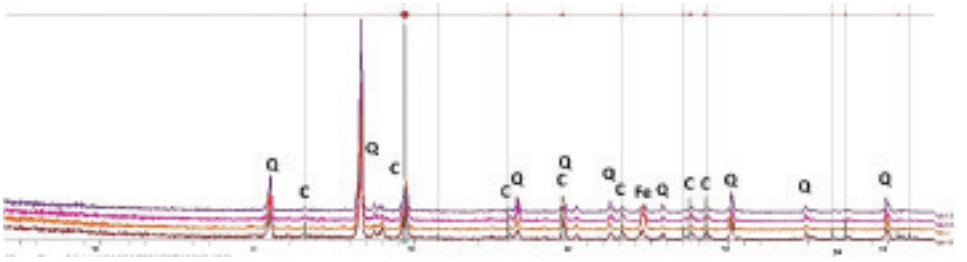

Fig. 7. Diffractograms of samples 1B, 2, 5A and 5B.

Tab. 2. Interpretation of X-Ray powder diffractograms. All mineral abundances are in %. Abundance of Fe is marked as "high" (++) and "low" (+).

	Sample			
	1B	2	5A	5B
SiO_2	68.6	71.3	75.0	77.7
$CaCO_3$	31.4	28.7	25.0	22.3
Fe	+	++	+	+

Calcimetry of powdered samples from boreholes 1B, 2, 5A and 5B (Tab. 3) shows the amount of dissolved $CaCO_3$ and insoluble residuum in the analysed samples. The insoluble fraction is SiO_2, which was determined by X-Ray diffraction. The largest amount of $CaCO_3$ was determined in the sample 1B and the lowest in the sample 5B.

Tab. 3. Results of calcimetry analysis. M1 = sample mass, M2 = mass of filter-paper, M3 = mass of filter-paper with insoluble residuum, M4 = mass of insoluble residuum, M5 = mass of $CaCO_3$, %Si = percentage of SiO_2, %Ca = percentage of $CaCO_3$ in sample.

	M1	M2	M3	M4	M5	%Si	%Ca
1B	0.3256	0.6398	0.8617	0.2219	0.1037	68.1511	31.8489
2	0.3051	0.6310	0.8576	0.2266	0.0785	74.2707	25.7293
5A	0.3650	0.6561	0.9124	0.2563	0.1087	70.2192	29.7808
5B	0.3839	0.6793	0.9699	0.2906	0.0933	75.6968	24.3032

The abundances of SiO_2 and $CaCO_3$ in the analysed samples are determined with better precision by calcimetry than by X-Ray diffraction, although the differences are not significant (Tab. 4).

Tab. 4. Comparison of abundances (in %) of SiO_2 and $CaCO_3$ in the analysed samples by X-Ray diffraction (XRD) and Calcimetry (Calc). Calcimetry values from Tab. 3 are rounded on two decimals.

	Sample							
	1B		2		5A		5B	
	XRD	Calc	XRD	Calc	XRD	Calc	XRD	Calc
SiO_2	68.6	68.15	71.3	74.27	75.0	70.22	77.7	75.7
$CaCO_3$	31.4	31.85	28.7	25.73	25.0	29.78	22.3	24.3

Qualitative optical analysis of Lopar sandstones showed that they are composed primarily of angular quartz grains and poorly rounded chert and quartzite grains bonded by calcite cement. Numerous grains have microfractures and undulose extinction which indicates their origin from weathering of metamorphic rocks.

The Lopar sandstones are faunistically sterile, although they are often bioturbated by boring organisms which apparently invaded the sediment from the upper surface that must have been colonized.

RESULTS OF MONITORING 2018 - 2022

The duration of monitoring was different from that originally intended in 2018, because we wanted to enlarge the data base with new sites to provide better coverage of the area. The quadrant 2B was set in 2019, and quadrants 6, 7 and 8 were set in 2020. Consequently, the monitoring period lasted 1684 days for quadrants 1A, 1B, 2A, 5A and 5B, 1307 days for quadrant 2B, and 706 days for quadrants 6, 7 and 8 (Tab. 5). Table 5 shows the average measured depths of boreholes for each year of monitoring and the change of average borehole depth after the monitoring period (difference of initial and final measurement, Δ). The changes in borehole depths over time indicate retreat of the rock face, and consequently represent the amount of weathered rock material, which is a direct measure of weathering. Table 5 also provides calculated values of daily and annual weathering on 1 m^2.

Quartz sandstones have a more resistant lithology than sandy marls, and the measured intensity of annual weathering of sandstones ranges from 0.25 mm to 1.21 mm, whereas for sandy marls it is consistently 1.5 mm (Tab. 6).

Tab. 5. Average borehole depths for each year of monitoring (0-4). Total change of borehole depth (Δ) and the intensity of daily and annual weathering (mm).

	0	1	2	3	4	Δ	n	weathering	
Quadrant	2018	2019	2020	2021	2022	0-4	days	mm/day/m^2	mm/yr/m^2
1A	21.98	20.93	20.69	20.32	20.04	1.94	1684	0.00115	0.42049
1B	20.88	18.91	18.72	16.48	13.72	7.16	1684	0.00425	1.55190
2A	22.57	20.43	20.25	19.67	20.29	2.28	1684	0.00135	0.49418
2B*	-	22.62	21.86	22.17	21.73	0.89	1307	0.00068	0.24855
5A	20.67	17.55	15.74	14.48	13.59	7.08	1684	0.00420	1.53456

	0	1	2	3	4	Δ	n	weathering	
Quadrant	2018	2019	2020	2021	2022	0-4	days	mm/day/m^2	mm/yr/m^2
5B	20.44	18.45	17.54	16.86	16.12	4.32	1684	0.00257	0.93634
6#	-	-	18.85	17.57	16.51	2.34	706	0.00331	1.20977
7#	-	-	17.96	17.03	16.23	1.73	706	0.00245	0.89441
8#	-	-	14.78	14.62	14.22	0.56	706	0.00079	0.28952
Initial measurements on quadrants in 2018, * in 2019 and # in 2020									

Tab. 6. Intensity of weathering in the monitoring period.

Quadrant	Date set	Exposition to wind	Days of monitoring	Years of monitoring	Weathering (mm)	Annual weathering (mm/yr)
SANDSTONES						
1A	25.3.2018	W	1684	4.61	1.94	0.42
2A	25.3.2018	NE	1684	4.61	2.28	0.49
2B	5.4.2019	NE	1307	3.58	0.89	0.25
5B	25.3.2018	NE	1684	4.61	4.32	0.94
6	29.11.2020	E	706	1.93	2.34	1.21
7	30.11.2020	SW	706	1.93	1.73	0.90
8	30.11.2020	NE	706	1.93	0.56	0.29
SANDY MARLS						
1B	25.3.2018	N	1684	4.61	7.16	1.55
5A	25.3.2018	NE	1684	4.61	7.08	1.54

Monitoring of the intensity of weathering of sandstones and sandy marls on Lopar Peninsula over a duration of 2 to 4 years shows local differences which are caused by proximity of measurement quadrants to the coastline and exposure to prevailing winds, and lithological variability (Fig. 8).

The monitored quadrants 1, 2, 5, 7 and 8 are exposed to the bora wind (which blows from the coastal mountain range), whereas quadrant 6 is exposed to both to the bora and the sirocco (which blows from the open sea). The only quadrant protected from the direct wind is quadrant 1A.

Quadrants 7 and 8 were established at the same time, on the same lithology, at a distance of 800 m from each other, and 55 m of difference in altitude, and provided very different weathering values. The weathering on quadrant 7 is three times more intensive than on the quadrant 8, which is undoubtedly caused by the environmental conditions of their micro-locations. Quadrant 8 is placed in a forested area which buffers wind-blown sand from the Sahara beach and protects the rock exposures from sand-blasting. The efficiency of sand-blasting is evident as the paint of marking letters

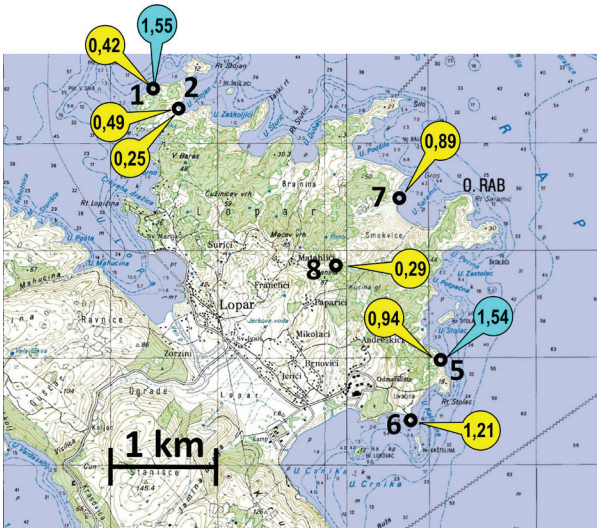

Fig. 8. Positions, lithology and measured annual intensity of weathering for monitored quadrants. Yellow balloons = sandstones, blue balloons = sandy marls.

on measuring sites was degraded and eventually completely destroyed in just a few months (Fig. 9).

From 2018 until the end of monitoring in 2022, most quadrants suffered significant selective weathering, the mouths of boreholes become irregular, which degraded precision of measurements, and in some cases completely disabled them. The rock faces of sandy marls were selectively weathered so that fossils and harder parts of the rock remained exposed whereas the matrix was weathered away, creating micro-topography which significantly increased measurement errors. Some rock faces also suffered exfoliation and/or mass wasting with collapse of the rock face slab along with the respective borehole (e.g. on quadrant 2B with borehole 5).

DISCUSSION

The intensity of weathering of Eocene sandstones and sandy marls is highly dependent of the position of the monitored quadrant relative to the coastline, so it is highest in the splash zone exposed to the bora wind. The intensity of weathering of sandy marls and sandstones attained the highest values of 1.54 mm (quadrant 5A) and 1.21 mm (quadrant 6) per year, respectively (Tab. 6), whereas it is much lower at quadrants located at greater distance from the coastline, or on the lee side (Fig. 8). In such protected locations it ranges between 0.25 mm/yr (quadrant 2B) to 0.94 mm/yr (quadrant 5B).

Sandy marls are subjected to desiccation and exfoliation, whereas mass wasting was controlled by the amount of clay in the matrix and the number of fissures and fractures.

Sand blasting was proven to be a very efficient weathering agent, as the painted quadrant identification letters were significantly, and some completely, eroded after 2-3 months of exposure on the rock face (Fig. 9), and some boreholes were filled with wind-blown sand.

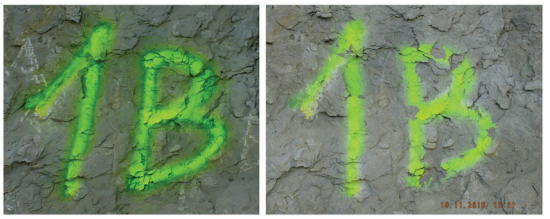

Fig. 9. Lettering on the polygon 1B is severely degraded in 94 days of exposure, and had to be repainted during each measurement campaign.

The measured intensity of the weathering of Lopar clastics indicate; a) the change in topography as a result of loss of the volume of exposed rocks, b) the rate of production of sand due to weathering of sandstones and sandy marls, and c) the amount of retreat of the exposure faces.

The most important weathering processes were; a) sand-blasting, namely abrasion of the exposures by wind-blown quartz sand, b) leaching of calcite cement which bonds debris in sandstones, and c) desiccation of clays in matrix of sandy marls.

The intensity of sand-blasting is dependent on the direction of the prevailing winds, and the amount of loose sand which forms aeolian deposits of the Lopar coves and can be remobilized by wind. However, monitoring over a duration of 4 years provides a record of the cumulative effect of all the winds that have been blowing in that period, and the field experience shows that on a local scale the wind direction was very variable due to topography of the peninsula.

In the modern climate, as indicated by the results of monitoring the weathering of sandstones is in average 0.64 mm/yr, and 1.5 mm/yr of sandy marls. If we extrapolate these values to the period of 100 years, the erosion of sandstone topography would reach 64 mm, whereas in 1000 years it would attain 640 mm. Erosion of sandy marls in 100 years would reach 150 mm, and in 1000 years 1500 mm.

If we assume even weathering of sandstones with 75.7% of SiO_2 on the surface of 100 m^2, the production of quartz sand would be 84.25 - 188.57 kg/yr, which depends on exposure of the weathered surface and local intensity of weathering (Tab. 6), or 8425.41 - 18856.67 kg/100 yr. Sandy marls with 70.2 % SiO_2 (the amount of quartz varies between 68.2% and 70.2%) yield for a surface of 100 m^2 286.49 kg/yr, or 28648.62 kg/100 yr. Sandy marls, though with lower amount of SiO_2. provide more quartz sand due to their higher intensity of weathering, which is caused by easier weathering of clay matrix compared with calcite cement in sandstones.

The above amounts of produced sand are minimalistic estimates, since they are based on the sand production from just 100 m^2, whereas in the real world we must take into account also drainage basin in hinterland with an area of ca. 1 km^2.

The retreat of coastal topography is a direct consequence of the intensity of the weathering of exposed rocks. The cemented sandstones experienced erosion of 0.42 m to 0.94 m in 1000 years, or 0.84 m to 1.88 m in 2000 years, which means than not one stone inscription from Roman times could be preserved. The retreat of cliffs made of sandy marls, which are more subjective to weathering, might have been ca. 1.5 m in 1000, or 3 m in 2000 years.

The intensity of weathering is strongly controlled by the distance from the coastline, so it is expectedly highest in the splash zone (quadrants 5A and 6), and lowest at a distance over 0.5 km from the coast (quadrant 8) in a forested environment. It may be concluded that the Lopar forest, which is about 50 years old, lowered the intensity of weathering by buffering wind-blown sand, and decreased the supply of sand to Lopar beaches relative to the previous period when the topography was barren bad-lands.

CONCLUSIONS

In 1684 days of monitoring, 7.08 - 7.16 mm of sandy marl was eroded, which corresponds to an annual weathering of 1.54 - 1.55 mm. Quartz sandstones are more resistant, and 1.94 - 4.32 mm was eroded in the same period, which corresponds to annual weathering of 0.42 to 0.94 mm. The quadrants monitored for 706 days showed weathering of 0.56 - 2.34 mm, which corresponds to an annual weathering of 0.3 - 1.2 mm.

The weathering of Eocene sandstones on Lopar peninsula is the combined result of a) leaching of calcite cement and b) sand-blasting by wind-blown quartz sand released from sandstones. It is larger in the marine splash zone exposed to the bora wind than in forested zones and zones at a greater distance from the sea and sources of loose sand.

The measured weathering intensities are strongly dependant on lithological variability, micro-locations of quadrants, their distance from the coastline, and the degree of shelteredness from wind and splashing.

Weathering of Lopar Eocene sandstones and sandy marls produces sand which deposits in coves and bays forming beaches and sandy shoals. Anthropogenic afforestation decreased the intensity of erosion by reduction of sand-blasting in the hinterland of beaches, which is about 3 times lower than in the sea splash zone.

Seasonal variations of the weathering intensity were poorly expressed, because periods of enhanced erosion were documented both in warm and cold months.

Monitoring of weathering on the Lopar measuring quadrants had to be abandoned after 4 years, because the rock faces become too irregular due to selective erosion and rock wasting to allow measurement of borehole depths with any precision. In some cases, the measurement became impossible because of the disappearance of boreholes, which may have been mass-wasted, or completely filled with wind-blown sand.

Weathering of Eocene sandstones and sandy marls created the topography of Lopar Peninsula by retreat of the exposure faces, and the amount of retreat depends on local lithological variability.

ACKNOWLEDGMENTS

This paper is an outcome of the research project “Geološka istraživanja erozijskih procesa na području značajnog krajobraza Lopar” awarded to ProGEO-Croatia by Public Institution Priroda of Primorje-Gorski kotar County in Rijeka, which was conducted in 2018-2022. We thank Director of Public Institution Priroda Marko Modrić, who granted permission for the publication of our research results. We are indebted to prof. Nenad Tomašić of the Division of Mineralogy and Petrography of the Department of Geology, Faculty of Science, University of Zagreb for his help with X-Ray diffraction research. We are also indebted to prof. Petra Peharec of the Division of

Molecular Biology, Department of Biology, Faculty of Science, University of Zagreb, who kindly admitted us into their laboratory for our chemical research.

Received January 24, 2024

REFERENCES

Altomare, A., Corriero, N., Cuocci, C., Falcicchio, A., Moliterni, A., & Rizzi, R., 2015: QUALX2.0: a qualitative phase analysis software using the freely available database POW_COD. Journal of Applied Crystallography **48**, 598-603.

Benac, Č., Ružić, I. & Žic, E., 2006: Ranjivost obala na području Kvarnera. Pomorski zbornik **44**(1), 201-214.

Benić, J., 1983: Vapnenački nanoplankton i njegova primjena u biostratigrafiji krednih i paleogenskih naslaga Hrvatske. Doctoral Thesis. University of Zagreb, 159 pp.

Bognar, A., Blazek, I., Tomulić, I. & Turk, H., 1989: Geomorfološke osobine otoka Raba. Geografski glasnik **51**, 7-20.

Bouma, A.H., 1969: Methods for Study of Sedimentary Structures. X+458, Wiley-Interscience, John Wiley & Sons, New York.

Haq, B.U., Hardebol, J. & Vail, P.R., 1987: Chronology of Fluctuating Sea Levels Since the Triassic. Science **235**, 1156-1166.

Katalinić, M., 2019: Modeliranje vjetrovnih valova u Jadranskom moru za primjene u brodogradnji i pomorstvu. Doktorski rad, Fakultet strojarstva i brodogradnje, Sveučilište u Zagrebu, 143 p.

Katalinić, M. & Parunov, J., 2014: Pregled klimatskih prilika u Jadranskom moru. In: Conference proceedings of the 21st symposium Theory and practice shipbuilding, in memoriam prof. Leopold Sorta, 555-562.

Lihoreau, F., Marjanac, L., Marjanac, T., Erdal, O. & Antoine, P.-O., 2003: A Late Eocene palaeoamasiine embrithopod (Mammalia, Afrotheria) from the Adriatic realm (Island of Rab, Croatia). Palaeovertebrata **47**, 1-11.

Mamužić, P., 1962: Novija geološka istraživanja otoka Raba. Geološki vjesnik **15**(1), 121-141.

Mamužić, P., Milan, A., Korolija, B., Borović, I. & Majcen, Ž., 1969: Osnovna geološka karta SFRJ 1:100.000, List Rab L 33-114, Institut za geološka istraživanja Zagreb, Savezni geološki zavod, Beograd.

Mamužić, P. & Milan, A., 1973: Osnovna geološka karta SFRJ 1:100.000, Tumač za list Rab L33-144, 5-39, Institut za geološka istraživanja Zagreb, Savezni geološki zavod, Beograd.

Marjanac, T. & Marjanac, Lj., 1999: Eocene clastics of the Rab island - Lopar peninsula, Rab. In: Some Carbonate and Clastic Successions of the External Dinarides. Harold Reading's I.A.S. Lecture Tour '99, Field-trip guidebook, 29-51.

Marjanac, T. & Marjanac, Lj., 2004: Stop 2.1: Eocene incised valley fill clastics of the island of Rab. Adriatic-Dinaric Mesozoic carbonate platform, environments and facies from Permian to recent time. 32th International Geological Congress, Florence 2004, Field-trip guidebook - P53, 16-21.

Marjanac, T. & Marjanac, Lj., 2007: Sequence stratigraphy of Eocene incised valley clastics and associated sediments, Island of Rab, Northern Adriatic Sea, Croatia. Facies **53**, 493-508.

Mitchum, R.M.Jr. & Van Wagoner, J.C., 1991: High-frequency sequences and their stacking patterns: sequence-stratigraphic evidence of high-frequency eustatic cycles. Sedimentary Geology **70**, 131-160.

Muldini-Mamužić, S., 1962: Mikrofaunističko istraživanje eocenskog fliša otoka Raba. Geološki vjesnik **15**(1), 143-159.

Ružić, I. & Benac, Č., 2016: Ranjivost obala otoka Raba zbog rasta razine mora. Hrvatske vode **24**, 203-214.

Ružić, I., Tadić, A. & Benac, Č., 2023: Erosion and vulnerability of beaches in Lopar peninsula (Rab Island, Croatia). 4th Scientific-expert conference Adaptations to Climate Change and Preservation of Marine Ecosystems of the Adriatic Sea with international participation. Krk Island, Croatia. Book of Abstracts, 19-20.